Twentieth European Rotorcraft Forum
Amsterdam, The Netherlands, September 1994

Smart Internal Blade Vibration Suppressor A Feasibility Study

J.P. Narkiewicz[1], G.T.S. Done
City University, London, UK

Abstract

The concept of a vibration suppression device mounted inside the rotor blade of a helicopter is considered.

First, the possibility of reducing vibration level by applying only dynamic type loads is examined. An optimization technique is used to provide the most effective parameters of applied loads. It is shown possible to obtain a reduction in vibration level by applying dynamic loads along the part of the blade span.

Next the concept of using an active "bender" type element mounted inside the blade and attached to the blade main spar for vibration suppression is studied. The bender is modelled as an elastic beam sandwiched on the longitudinal faces normal to the beam bending plane by layers of piezoelectric material. When an alternating voltage is applied to the piezoelectric layers, the element is excited into a bending motion, which leads to a dynamic force and moment reaction at the attachment point.

The performance of such a device is studied using a computer model of hingeless rotor blade. The bender placement and design parameters are varied in order to obtain the insight into their influence on the vibration suppression.

For the blade and bender parameters considered it appears that excitation by blade motion overrides the control available by the piezoelectric layers.

Notation.

b - width of the bender
c - blade chord
d_{31} - piezoelectric constant
E_p - modulus of elasticity of piezoelectric
J_{Fk} - vibration index based on k-th load
k - index for blade load components
L_D - applied dynamic force
M_D - applied dynamic moment
M_{nl} - moment in n-th bender segment for k-th mode
N - number of harmonics of additional load
R - rotor radius
t - time
t_{bn} - thickness of beam in n-th segment
t_{ln} - thickness of layer at n-th segment
$U_n(t)$ - voltage applied
U_T - blade tip speed
φ_0 - phase of applied load
ρ - air density
η'_{kT} - angle of deflection at the end of the bender segment for k-th mode
μ - advance ratio
ψ - azimuth angle
Ω - rotor angular velocity

1. Introduction.

As the crucial components on which helicopter performance and handling qualities depend are the main and tail rotors, so improvement of these elements leads to an enhancement of the overall rotorcraft quality. This provides the motivation for many investigations into the possibilities of smart structure applications in rotorcraft. A smart device is a controlled device

[1] On sabbatical from Warsaw University of Technology, Warsaw, Poland

and it is natural that the application to improvement of rotor control is mainly considered.

A long term goal of the application of smart structures is eliminating the existing swash-plate mechanism. It could be achieved by the designing of an integrated system which would perform simultaneously primary rotor control i.e. that control which achieves the trim and required flight state including manoeuvres, and eliminate the need for or perform additional rotor control used actually for improvement of performance by the elimination of flow stall regions, the alleviation of response to gusts and turbulence, the suppression of rotor and fuselage vibration or/and the reduction of noise.

Recently several different concepts of smart rotors have been investigated [1]. From the design point of view these are:

- tuning the dynamic properties of the rotor,
- adapting the blade shape to the ambient flight,
- operating some additional device mounted on the blades.

Shape adaptive blades can be constructed to change the blade twist, the shape of the blade cross-section, and the deflection in and out of the plane of rotation. Application of shape adapting blades directly to full scale rotors appears to be not currently possible because of insufficient actuating power and reliability of existing smart materials.

The loads on rotor blades can also be influenced by using leading or trailing edge control surfaces. The use of blade trailing edge tabs for primary control has been successfully implemented by Kaman in their products, most recently on the K-Max helicopter.

In the design of a trailing edge tab actuated by smart materials different driving mechanisms are concerned as the key factor. In many proposed solutions [2-4] a piezoelectric bender was used for controlling the tab. Tabs driven by piezoelectric benders were tested experimentally in [4] on a rotor model in hover.

Several analytical studies have been carried out to obtain insight into different aspects of the application of a trailing edge tab. The use of tabs for primary control was investigated in [5], for vibration suppression in [6], for blade vortex interaction reduction in [7] and for rotor performance optimisation in [8].

Physical phenomena involved in "smart tab" applications are both dynamic i.e. involving inertia and elastic loads, and aerodynamic. Up till now only effect of aerodynamic influence on rotor behavour has been investigated. The influence of blade motion on the actuating device has not been considered yet.

The aim of this study, as a part of a wider project, is to explore the possibility of reducing blade vibration level by dynamic activity only, avoiding interference with the aerodynamic environment. The anti-vibration device is designed as a smart element mounted inside the blade.

The possibility of diminishing vibration level by applying non-specific "dynamic type" loads at a selected part of blade radius is explored first using an optimization technique for parametric study. The index of vibration level is based on loads at the blade root in a rotating frame of reference.

In the second part of the study the coupled motion of blade and internally mounted bender is explored to reveal the possibility of direct application of this kind of device. The possibility of influencing the motion of the bender by actuating smart layers is studied. This investigation gives indications for designing bender type driving mechanisms for actuating trailing edge tabs.

2. The scope of the study.

The topics considered in this study are:
a) the development of a computer model of the bender type device,
b) the incorporation of a smart bender into the blade model,
c) the possibility of suppressing blade vibration by applying only dynamic loads,
d) the exploration of the behaviour of the blade with a blade mounted vibration suppressor.

3. Bender model.

The active element comprises a "bender", i.e. a elastic beam element, attached to the blade main spar, mounted inside the external envelope of the aerofoil (Fig.1). It is sandwiched on the longitudinal faces normal to the beam bending plane by layers of smart material. When an alternating voltage is applied to the layers, the element is excited into a bending motion, which leads to a dynamic force and moment reaction at the attachment point. To operate effectively the dynamic loads at its root should produce an adequate force and twisting moment about the elastic axis of the blade.

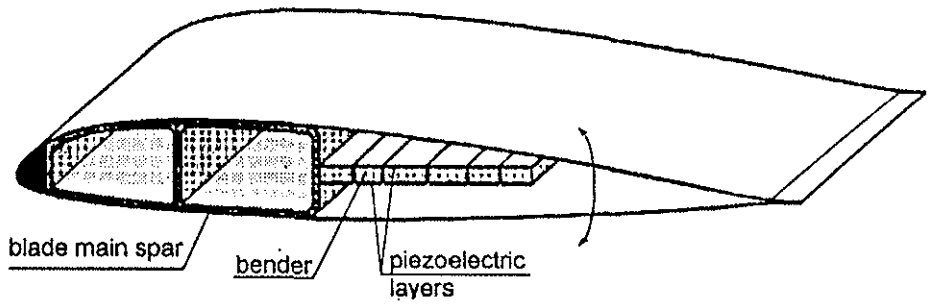

Fig.1. The bender type vibration suppressor mounted inside the blade.

For the needs of this and other related studies the computer model of a multielement beam type bender was developed. In comparison with a one element device this allows greater freedom to chose bender dynamic properties and to control the deflections by supplying voltages to each segment.

The assumptions used in the bender computer model are:
1. The bender comprises a cantilevered beam divided into N segments of different lengths.
2. The materials of beam and smart layers are isotropic and uniform.
3. Segments are connected stiffly i.e. adjoining elements have the same deflections and rotations at the interfaces.
4. Each segment is treated as a separate Euler-Bernoulli beam.
5. The upper and lower surfaces of each segment may be covered by a layer of smart material.
6. The distances between the layers of adjoining segments are negligible, but large enough to prevent contact of the layers during deformation.
7. Viscous damping for each segment mode is assumed.

The Lagrange equations of motions are derived and the normal mode equations for each segment are obtained by the Galerkin method.

The external load for each segment, resulting from beam/layer interaction is calculated using the model described in [10] for the piezoelectric layers. The external bending moments from the piezoelectric layers in each segment equations of motion are calculated as:

$$M_{af}=2\eta'_{IT}bd_{31}E_p(t_{ba}+t_{ln})t_{ba}U_a(t) \qquad (1)$$

where the symbols in (1) are defined in the Notation.

4. Blade model.

A single blade of a helicopter rotor in steady flight is studied. The angular velocity Ω of the rotor shaft is constant.

For the blade modelling a well tried and tested computer model of an individual blade is utilized, which is described fully in [10]. This model allows the selection of different arrangements of hub hinges and deflection modes of the blade.

The base blade configuration selected for this study comprises the deformable blade attached to the shaft via a stiff element having lag offset. It can be controlled in pitch about a feathering bearing.

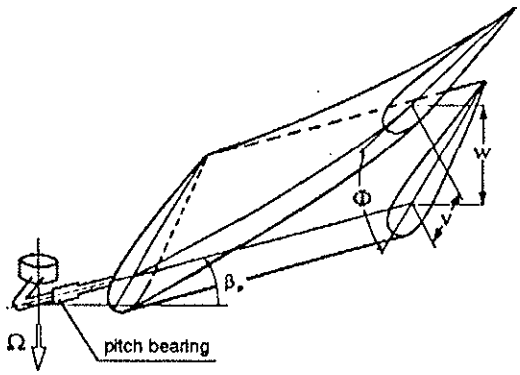

Fig.2. Base blade model: lag-wise, flap-wise and twist deflections.

The blade has a straight elastic axis and is pretwisted about it. It can bend lag-wise, flat-wise and twist about the elastic axis. The blade cross sections have symmetry of elastic properties about the chord and there is no section warping. The blade stiffness loads are obtained from a Houbolt-Brooks model. Viscous structural damping of blade deformations is included in the model. The blade deflections are discretized by free vibration modes.

The aerodynamic loads are calculated from a two-dimensional, quasi-steady, nonlinear model based on a table look-up procedure. The induced velocity is calculated from the Glauert type formula.

The vector of blade motion generalised coordinates contains elastic degrees of freedom resulting from discretization of blade deformations by normal modes. In the case considered, for each type of blade deformation (i.e. flap, lead-lag and twist), one rotating normal mode is taken.

Gear's algorithm is used for numerical integration of equations of motion, which allows solution of "stiff equations".

In the case when blade steady motion is required, the equations of blade motion are integrated for a prescribed number of rotor revolutions. The steady values of blade deflections or loads are taken to be the values achieved during the last rotation.

Numerical results are obtained using as the base data that of the Westland Lynx blade [11]. The main values of blade parameters are given in Table I.

Table I. Blade base data.

rotor radius	6.40 m	blade lenght	5.61 m
lead-lag offset	0.025 m	blade chord	0.395 m
angular velocity	34.17 rad/s	blade mass	57.16 kg
flap mass static moment	121.61 kgm	flap inertia moment	437.54 kgm^2

linear twist 4.3° at the root, -2.2° at the tip

deformation	frequency 1/rev	damping %
lag	0.656	1
flap	1.087	3
twist	6.298	1

The base flight conditions concern an untrimmed rotor with collective pitch control of 13° and no cyclic control. The flow velocity expressed as rotor advance ratio varies from 0 to 0.35 in 0.05 intervals. The air density $\rho = 1.225\ kgm^{-3}$.

5. Requirements of performance for vibration suppressor.

In this section of the paper the activity described is aimed at assessing the possibility of reducing vibration levels by applying pure dynamic loads along the part of blade span. The influence of the vibration suppressing device on the blade is modelled as a normal force L_D and twisting moment M_D distributed locally over part of the blade span. The values of these loads are varied in such a way as to diminish the blade vibration level.

A blade vibration level index is used which is based on the loads acting at the blade root. In general terms it is defined as the difference between required and actual loads measured at a chosen point.

The values of required blade loads can be determined from consideration of overall helicopter trim or they can arise from the need to reduce a particular load component and/or one of its harmonics.

In this study, the indices of vibration level are defined for each component of blade load individually. They are calculated for blade steady motion during one rotor rotation as the average difference between the required and actual values of a selected load component, relative to the required loads according to (2) at M azimuth stations.

$$J_{Fk} = \frac{\sum_{i=1}^{M} |(F_{k0}(\psi_i) - F_k(\psi_i)|}{\sum_{i=1}^{M} |F_{k0}(\psi_i)|} \qquad (2)$$

$$\Delta J_{Fk} = \frac{J_{Fk0} - J_{Fk}}{J_{Fk0}} \qquad (3)$$

To evaluate the improvement in vibration suppression, the relative performance index ΔJ_{Fk} is calculated according to (3), where J_{Fk} corresponds to the end of computations and J_{Fk0} is the value calculated at the start of computations.

The value of the indices J_{Fk} depends on the flight conditions and design parameters of the blade and vibration suppressor. To assess the possibility of reducing the overall vibration level, a parametric study of the influence of all parameters should be performed. To avoid calculation of large number of cases during parametric studies, an optimization procedure is utilized to obtain the most suitable sets of design parameters.

The method selected to fulfill this task is the Powell algorithm, described in [11]. This is a non-gradient method, using the concept of a penalty function with selfadjusting direction and step size in searching for the minimum of the quality index. This algorithm forms a part of computations performed to obtain the final values of performance index in (2) or (3)

An optimization constraint arises by assuming that the thrust coefficient must not vary more than a prescribed fraction of the basic value. Imposing this constraint is necessary in order to prevent minimizing the vibration level to zero by application of very high additional loads.

For the assumed blade model and helicopter flight conditions the sequence of calculations for finding optimal values of additional loads is:

1. Compute the blade base loads $F_k(\psi_i)$.
2. Calculate the steady motion of the blade without additional loads.
   The blade steady loads obtained at this stage are used to calculate the starting value of the vibration index and the value of the rotor thrust coefficient to constrain the optimization process.
3. Use the optimization algorithm to calculate the values of variables minimizing J_k for selected k.
   Each step of the algorithm contains the calculation of blade steady motion.
4. When the optimization process is completed, the blade steady motion is calculated using the computed optimal parameters.

For this part of the study the additional loads are dependent on time (azimuth) in the form (4) and are distributed along part of the blade span.

$$M_D=\sum_{n=0}^{N} A_{Dn}\cos(\psi n+\varphi_{0n}) \qquad L_D=\sum_{n=0}^{N} B_{Dn}\cos(\psi n+\varphi_{0n}) \tag{4}$$

The optimization variables in the order of application in the algorithm are: amplitudes A_{Dn}, B_{Dn}, frequencies n and phase angles φ_{0n} of these loads. The sets of these parameters differ according to the case considered, as described below. Within the algorithm the order of searching values minimizing blade loads is first by applying the moment A_{Dn}, next force B_{Dn}, next changing frequency n, and finally φ_{0n}, which corresponds to static optimization first, and next dynamic i.e. changing forces in time.

The blade loads on the pitch controlled, non-deflecting blade are taken as the required load values F_k. This simulates the most stringent requirements for vibration reduction, since at the blade hub the only excited loads are no more than those actually required.

The results of three groups of computations are presented next. The additional loads are distributed starting from blade section 0.83R along a short length of span span of 0.2 m i.e. 0.032R.

I. The applied additional loads (4) have only one harmonic, i.e. N=1. The same frequency and phase angle is assumed for the additional moment and force. This assumption reflects the fact that prospective common sources of these loads result from the same inertia forces.

The results obtained for the base blade model are presented in Fig.3. A typical plot in Fig.3 shows the change in relative performance index ΔJ_{Fk} based on, for example, lateral force resulting from the rquirements of minimizing each of six components at the blade root. The separate curves are not individually identified because it is the general trend of the curves collectively which is important.

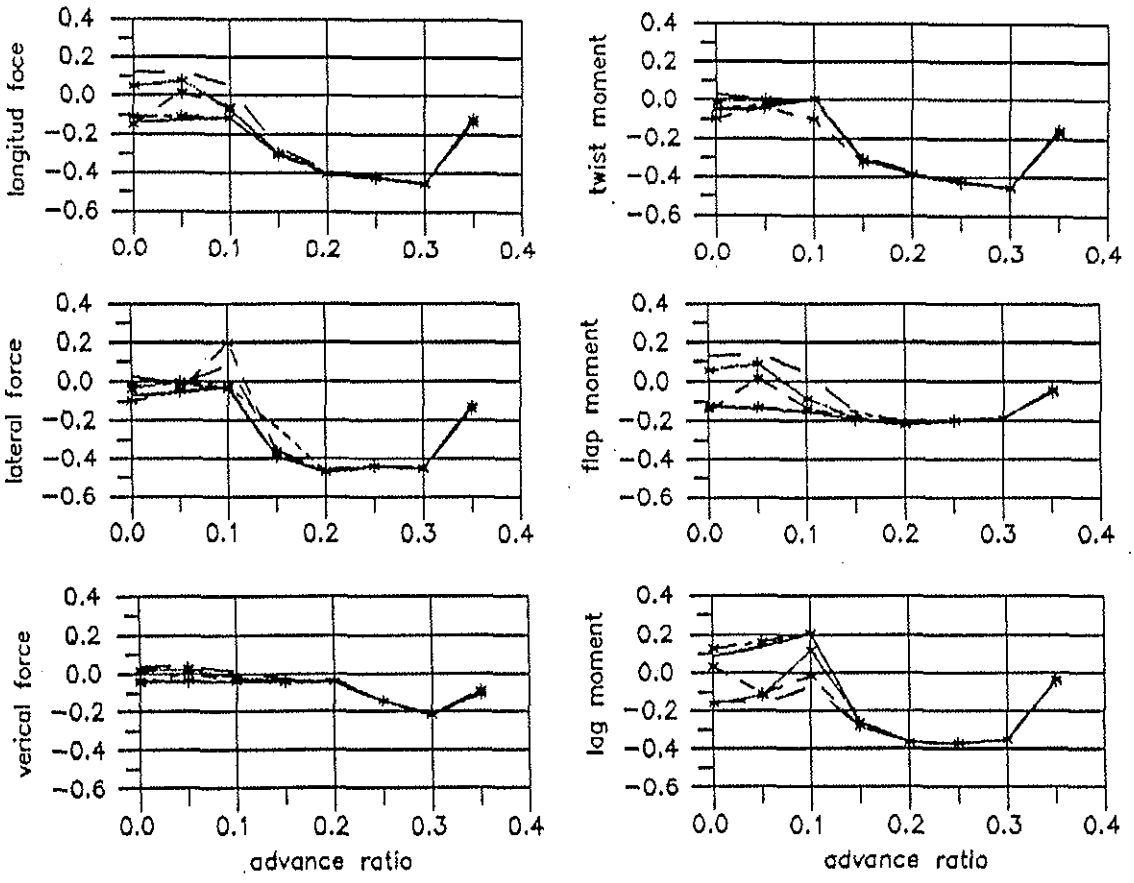

Fig.3. Change of performance indices for blade root loads by optimizing selected components of resultant loads for fully elastic blade.

It can be concluded that minimization of one component of blade load also usually implies minimization of all other load components. Sometimes, even when optimization is unsucessful for an assumed load, the minimization of other components occurs. Some

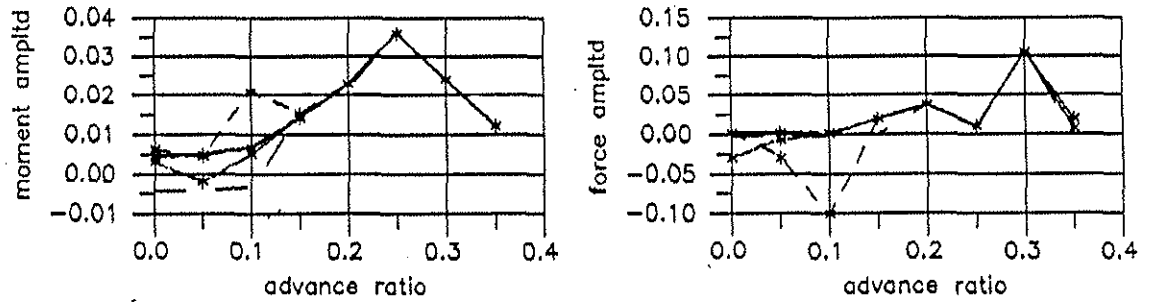

Fig.4. Amplitudes of the applied force and moment for the vibration indices in Fig.3

difficulties with vibration suppression at low-speed flight are apparent. For cruise flight an improvement in vibration level up to 40% of the base level can be achieved.

In the case considered, the optimization algorithm is able to perform only static optimization since almost no frequency and phase changes is produced by the algorithm (this is why they are not included in Fig.4). In Fig.4 the amplitudes of moment and force are nondimensionalized by dividing by $0.5\rho U_T^2 c^2$ and $0.5\rho U_T^2 c$ respectively.

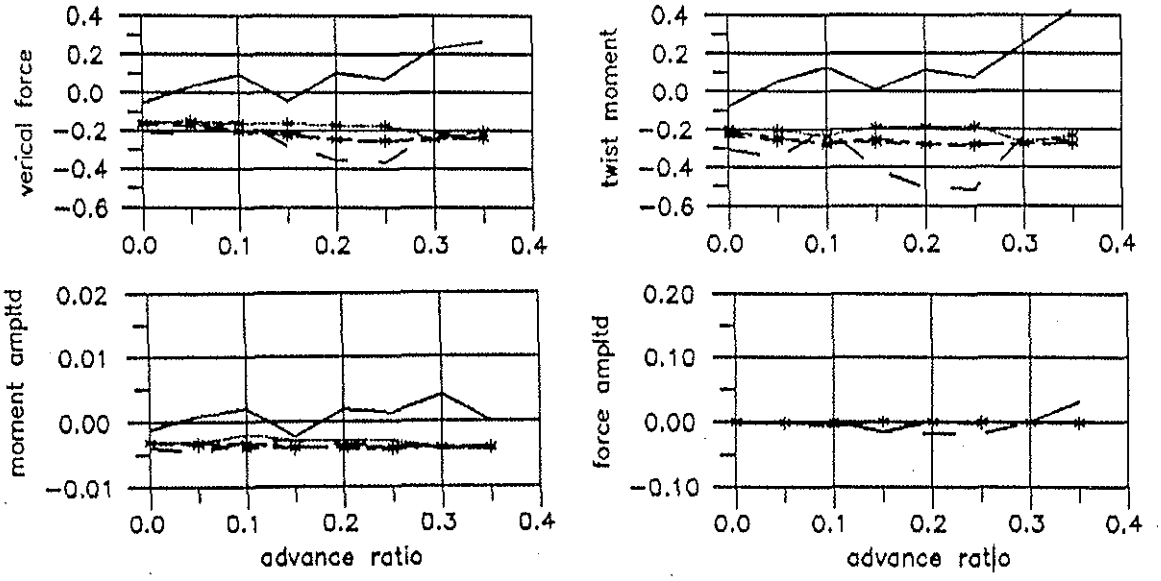

Fig.5. Change in vibration indices for the blade deformable flap-wise and rotating in pitch bearing.

Two other blade models are considered in this group of computations. One has as blade degrees of freedom rigid rotation at the pitch bearing and flapwise bending deflection, the other only blade torsion. These arrangements can be considered as models of special types of blades, for instance, in which selected deflections are suppressed.

For these blade models the results are not so consistent and some cases are unsuccessful in minimising the vibration index. In Fig.5 and Fig.6 the changes in resultant blade root vertical force and twisting moment are shown for these models.

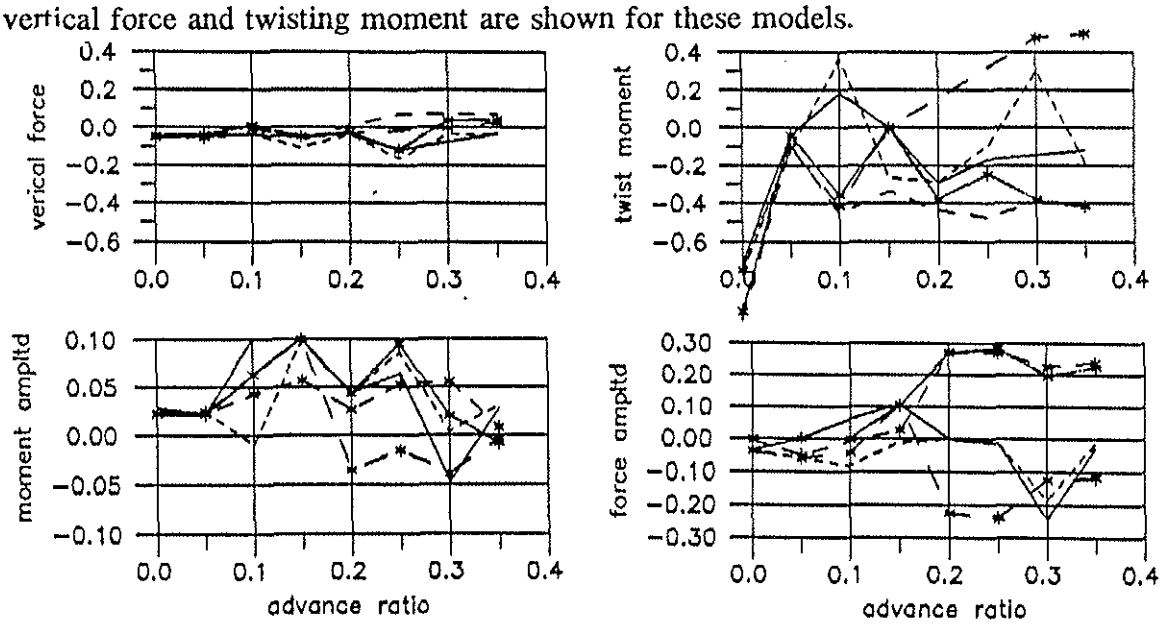

Fig.6. Change in vibration indices for the blade deformable in twist only.

Resulting from this part of the study, the normal force and twisting moment at the blade root are chosen for the next two groups of computations, being the components of blade load most directly influenced by additional load.

II. In the second case, loads at the blade root are minimized assuming constant exciting frequency for the additional force and moment. Frequencies 1, 2, 3, 4, 5 per rev are considered. The results for indices for the resultant vertical forces and twisting moments are shown in Fig.7.

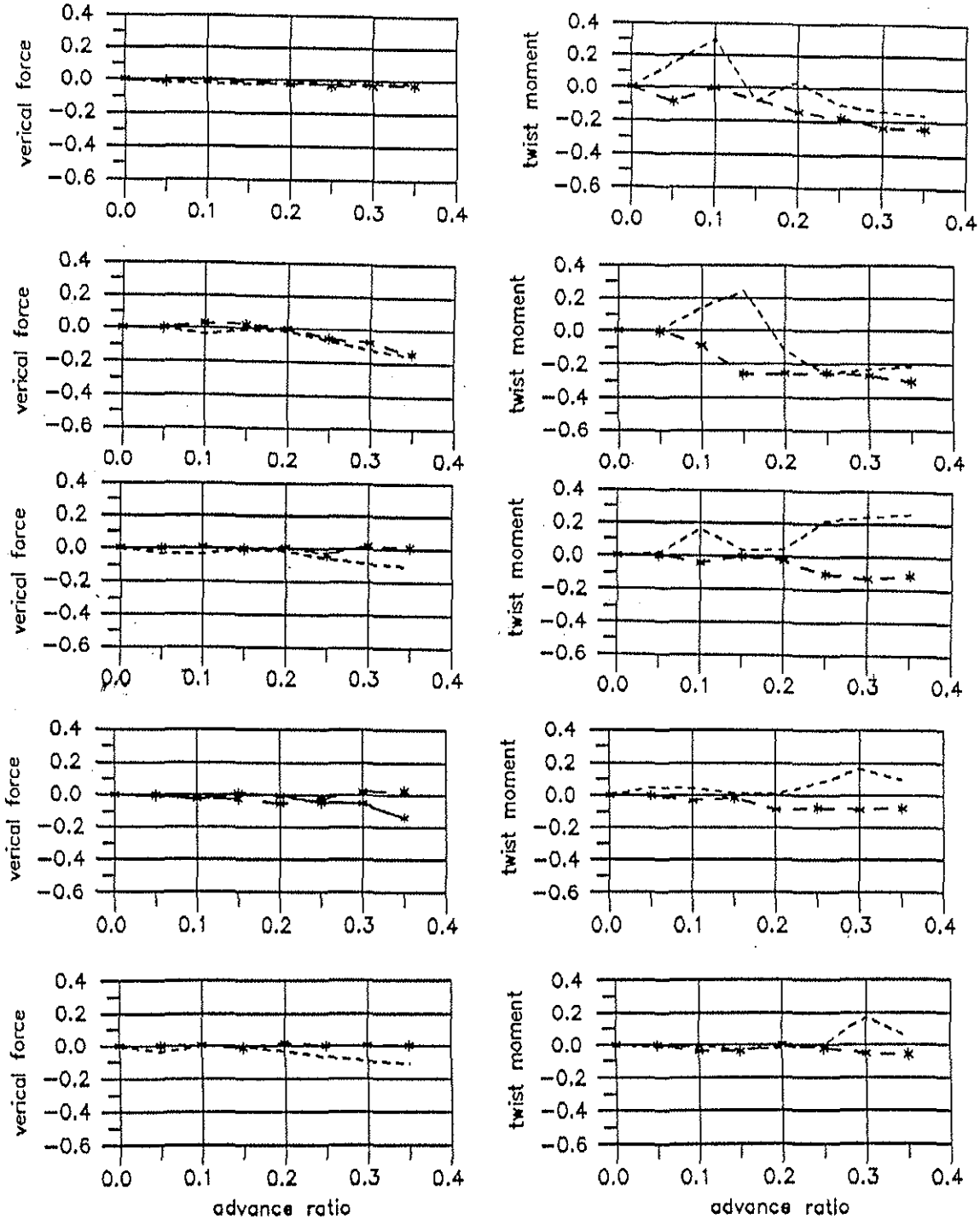

Fig.7. Change in performance indices for excitation by selected harmonics 1, 2, 3, 4, 5 per rev reading down the page. Base model.

For all cases the computed phase angles are inconsistent, which suggests that the algorithm does not behave well in dynamic analysis. The vibration index based on twisting moment (all the curves with the longer dashed lines) gives better vibration suppression for all load components. The application of the first and fifth harmonic does not seem to be efficient, compared with the 2, 3, and 4 per rev. The best results are obtained for excitations of 2 and 3 per rev, and the 4 per rev gives the smoothest function $J_{Fk}(\mu)$.

III. In the last case in this group of computations the additional loads are in the form:

$$M_D=\sum_{n=1}^{4} A_{Dn}\sin(n\psi+\varphi_n) \qquad F_D=KM_D \tag{5}$$

These formulae reflect the fact that, in the case of the dynamic suppressor, the common source of loads is inertia force. For a definite design of bender the relationship of inertia moment to inertia force is fixed. For the case of the bender considered in the next section $K=3.0\,m^{-1}$. The optimization parameters are the amplitudes and the phases of four harmonics of additional loads. The indices based on vertical force and twisting moment are shown in Fig.8 for minimizing each load at the blade root.

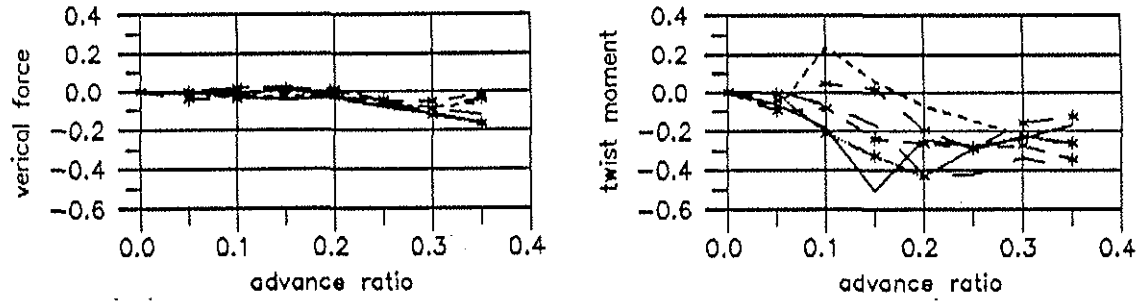

Fig.8. Change in vibration indices for "dynamic type" loads (5). Base model.

In this case, minimizing vertical force leads to an increase in vibration for twisting moment. The overall level of vibration suppression is less than in the previous cases.

The final conclusions which can be drawn from these three groups of calculations is as follows:

1. There is a potential possibility for diminishing the varying loads at the blade root by applying only dynamic loads along a part of the blade span.
2. These loads can be adjusted to minimize a selected blade root component.
3. The results of the minimization depend on the blade model considered, which implies, that each blade configuration should be analysed individually.
4. It is potentially possible by the minimization of one component of blade load to diminish the vibration level for all the other components.

The last conclusion provides an indication for designing control algorithms based on blade force measurement.

6. Blade with dynamic bender type device.

The aim of this part of the study is to explore the behaviour of a rotor blade with an embedded bender type device. The base blade arrangement described in Sec.4 is used here.

A single element bender attached to the blade main spar is considered, covered on both sides by piezoelectric layers.

The base bender data in this case are given in Table II.

Table II. Bender data.

		beam	layer
material		steel	PZT
Young's modulus	(Nm^{-2})	$21.6 \cdot 10^{10}$	$6.2 \cdot 10^{10}$
density	(kgm^{-3})	7800	7600
piezo coeff d13	(Vm^{-1})		$1.9 \cdot 10^{10}$
height	(m)	0.01	0.0005
width	(m)	0.2 (3.1%R)	full surface covered
length	(m)	0.25	0.25
number of modes		1	
mode shape		cantilevered beam	
damping	(%)	0.5	

The blade motion is studied for the following cases:

A. Blade without bender.

B. Bender mounted inside the blade, excited by the blade motion, with blade deflections unaffected by bender motion.

C. Coupled motion of blade with bender.

D. Coupled motion of blade with bender excited by harmonic voltage.

The results of computations are presented for the last rotor rotation of the series of rotations assumed for calculation of blade steady motion (i.e. after 9 revolutions). Twist angels are given in radians, tip displacements in meters.

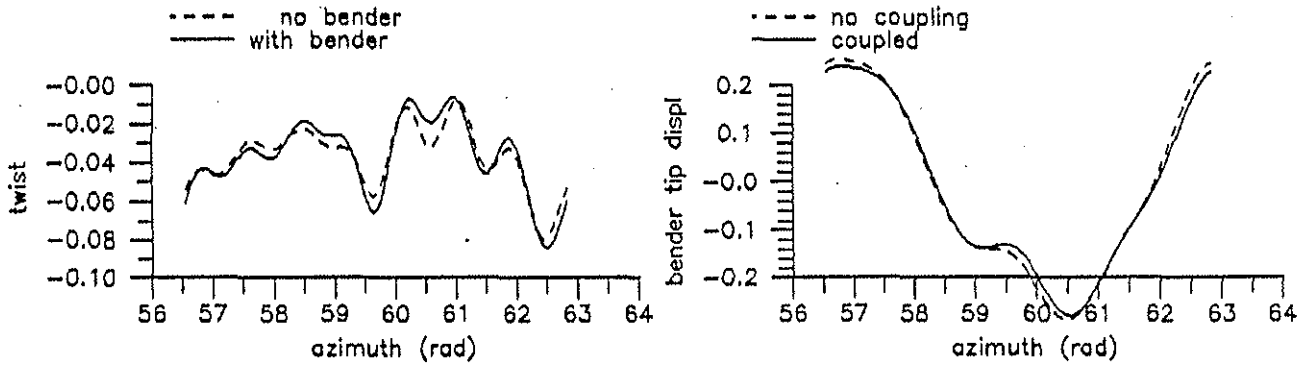

Fig.9. Influence of bender/blade dynamic coupling.

Comparing the blade motion for cases A and B (without and with bender mounted at radius 0.83R) no influence on blade flap and lag motion is observed. The influence of embedding the bender on blade twist angle and the bender tip motion for this case is shown in Fig.9. The deflections of the bender tip are unrealistically high, due to excitation from blade motion.

The attempt to influence the bender motion by exciting the piezoelectric layers harmonically at 1 per rev with a voltage amplitude 200V are shown in Fig.10 for blade twist and bender tip motion. The conclusions drawn from this result is that the bender has some slight influence on the blade twist deflection but the bender excited motion cannot be influenced by applying voltage to piezoelectric elements.

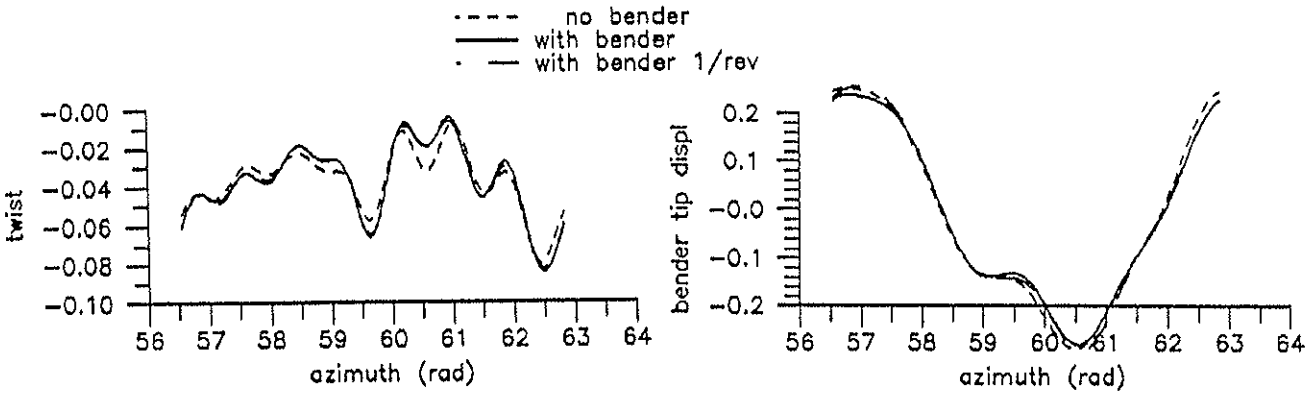

Fig.10. Influence of bender/blade dynamic coupling on possibility of excitation of bender motion.

The influence of advance ratio and bender radial position on the blade/bender motion is investigated next. The amplitudes of blade twist angles and bender tip deflections are shown in Fig.11 as functions of bender radial placement for different advance ratios. For constant advance ratio, blade twist amplitude does not depend on bender placement. Bender tip amplitude grows rapidly with radial distance from the shaft axis but stabilizes outboard of 0.25 R. It can be concluded then, there is a very narrow margin of blade placement radius and advance ratio within which the bender tip deflections are acceptable.

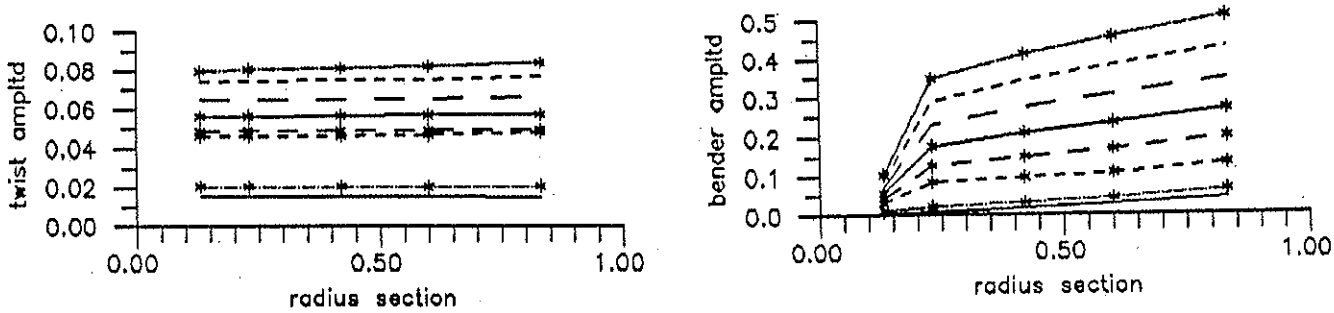

Fig.11. Influence of bender radial placement on amplitudes of blade twist and bender tip displacement.

The next case, Fig.12, illustrates the influence of cyclic pitch on bender motion for the bender placed close to the blade root at r=0.13R and for zero advance ratio. The blade collective pitch is 13° and the longitudinal and lateral cyclic pitch angles are varied. Two

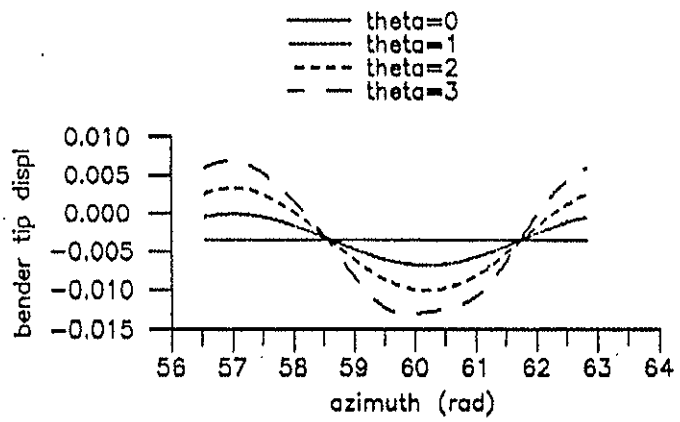

Fig.12. Influence of cyclic pitch on bender tip displacement.

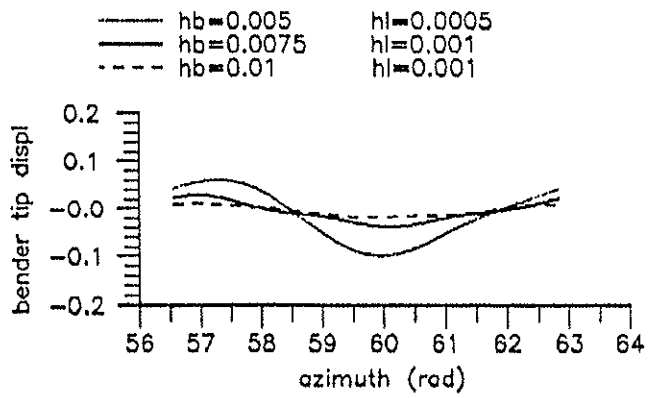

Fig.13. Influence of beam and layers thickness on bender tip motion.

cases are compared namely bender free and excited 1 per rev, 200V. The cyclic pitch excitation enables the bender motion to be influenced for the design parameters chosen.

Some results of a parametric study undertaken to investigate the influence the beam/bender thickness ratio on the possibility of influence the device motion are presented in Fig.13. For all cases it was impossible to stabilize bender motion, even when applying a higher voltage of 600 V.

Conclusions.

From the current study it can be concluded, that:

1. The concept of suppressing vibrations by applying only dynamic loads along part of the blade span can lead to substantial vibration reduction in terms of blade root loads.
2. Suppressing one load component can lead to suppression the others. This result may be useful both for vibration suppression concept and control system design.
3. A bender type device mounted inside the blade is subjected to considerable excitation due to blade motion. Attempts to reduce this excited motion by PZT layers turned out to be unsuccesful.
4. Blade cyclic pitch can be regarded as the main factor causing excessive bender movement.

The results have implications for the use of bender type devices in operating blade mounted tabs.

Acnowledgments.

The present work forms a part of a research programme funded by UK EPSRC on "Application of Smart Structures to Helicopter Rotor Blade Design".

References

1. Narkiewicz J.P., Done G.T.S., "An Overview of Smart Structure Concepts for Helicopter Rotor Control", to be presented at Second European Conference on Smart Structures and Materials, Glasgow, October 1994.
2. Strelhow H., Rapp H., "Smart Materials for Helicopter Rotor Active Control", AGARD/SMP Specialist's Meeting on Smart Structures for Aircraft and Spacecraft, 5-7 October, 1992, Lindau, Germany.
3. Straub F.K., "A Feasibility Study of Using Smart Materials for Rotor Control", 49th American Helicopter Society Forum, St.Louis, Mo, May 1993.
4. Chopra I.,"Development of Smart Rotor", Pap. No. N6, XIX European Rotorcraft Forum, Cernobbio (Como), Italy, Sept. 1993.
5. Yillikci Y.K.,"Aeroelastic Analysis of Rotor Blades with Flap Control", Paper No. E04, XIX European Rotorcraft Forum, Avignon, September 1992.
6. Millot T.A., Friedmann P.P., "The Practical Implementation of an Actively Controlled Flap to Reduce Vibrations in Helicopter Rotors", 49th American Helicopter Society Forum, May 1993, St. Louis, Mo, USA.
7. Straub F.K., Robinson L.H., "Dynamics of a Rotor with Nonharmonic Control", 49th American Helicopter Society Forum, St.Louis, Mo, May 1993.
8. Narkiewicz J., Rogusz M., "Smart Flap for Helicopter Rotor Blade Performance Improvement", XIX European Rotorcraft Forum, Como, Italy, Sept. 1993.
9. Meressi T., Paden B., "Piezoelectric Actuator Design for Vibration Suppression: Placement and Sizing", Journal of Guidance, Control and Dynamics, Vol.16, No.5, Sept-Oct.1993.
10. Narkiewicz J., Lucjanek W., "Generalized Model of Isolated Helicopter Blade for Stability Investigation", XVI European Rotorcraft Forum, Glasgow 1990, Pap. No. III.8.2.
11. Lau B.H., Louie A.W., Griffiths N., Sotiriou C.P.,"Performance and Rotor Loads Measurements on the Lynx XZ170 Helicopter with Rectangular Blades", NASA TM 104000, May 1993.
12. Kreglewski T., Rogowski T., Ruszczynski A., Szymanowski J., "Optimization methods in FORTRAN", (in Polish "Metody optymalizacji w jezyku FORTRAN"), PWN, Warszawa, 1984.